Physics practical report

Shanil Shah sbs57
Part IB Physics Report

December 6, 2025

Abstract

1 Introduction

Transformers form a core part of modern technology, being used for impedance matching within electronics and electricity transmission on the grid. In both systems, the efficiency and performance are determined by how the transformer responds to an applied magnetic field.

This response is described by the relationship between the magnetic flux density B and the magnetising field H, known as the B-H curve. By altering the core of the transformer its properties can be changed. For ferromagnetic materials, the B-H curve is non-linear and exhibits hysteresis (**Figure 1**) due to magnetic subdomains in the material.

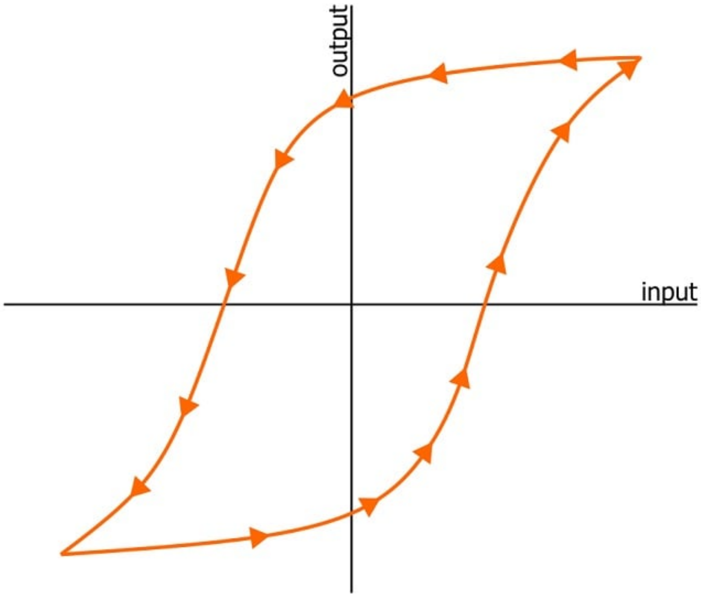

Figure 1: A typical hysteresis curve for a ferromagnetic material, showing the relationship between B and H. [1].

The most efficient transformers are made by having a high magnetic susceptibility (μ_r) and low energy loss per cycle. This experiment aims to quantify the usability of different materials as transformer cores, by measuring the energy loss per cycle per unit volume (given by the area of a hysterysis loop) and the maximum magnetic susceptibility (given by the gradient). Section 2 of this report will go through the relevant theory. Section 3 outlines the experimental setup, and Section 4 shows the results obtained. This data is analysed and compared against theoretical expectations in Section 5. The overall conclusions are then presented in Section 6.

2 Theoretical background

2.1 what is hysterysis

Hysterysis is the phenomenon where the value of a physical property lags behind changes in the effect causing it. In magnetic materials, this is observed as a lag between the magnetisation of the material and the external magnetic field applied to it. This results in a hysteresis loop when plotting magnetic flux density B against magnetic field strength H. there are 3 key points on the hysterysis loop these are shown in Figure 2.

- **(A) Saturation magnetisation** (B_{sat}): This is the maximum magnetic flux density that the material can achieve. Beyond this point, increasing the external magnetic field H does not significantly increase B.
- **(B) Remanent magnetisation** (B_r): This is the magnetic flux density that remains in the material when the external magnetic field H is reduced to zero.
- **(C) Coercive field** (H_c): This is the magnitude of the reverse magnetic field that must be applied to reduce the magnetic flux density B to zero after the material has been magnetised to saturation.

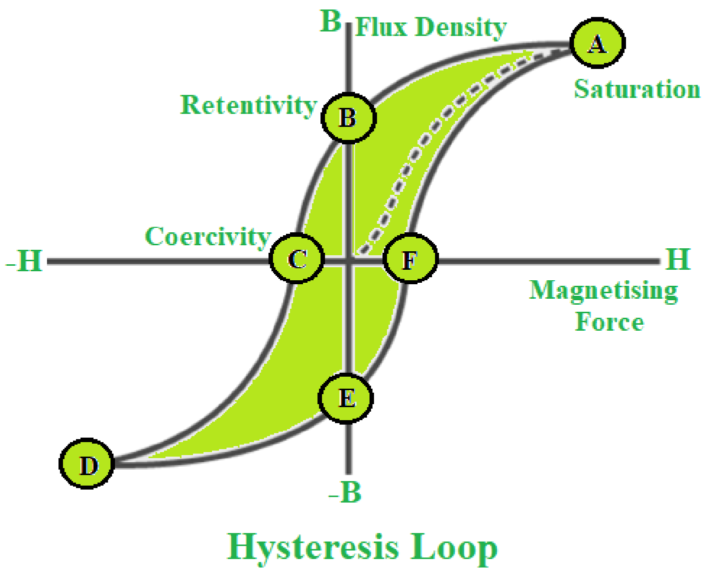

Figure 2: Labeled hysterysis loop [2].

Hysterysis is caused by the magnetic domains within the material. When an external magnetic field is applied, these domains tend to align with the field, increasing the overall magnetisation of the material. However, due to imperfections in the material and interactions between domains, they do not realign instantaneously. This time delay is visible as when the external field is changed, the magnetic domain are miss aligned and have to absorb energy to realign themselves causing energy loss in the form of heat.

2.2 workings of a transformer

The magnetising field H inside a solenoid is given by

$$H = \frac{nI}{L} \tag{2.1}$$

Where n is the number of turns, I the current, and L the solenoid length.
This gives rise to the magnetic flux density B For solenoids, with non-magnetic media in their core, there is a linear relationship:

$$B = \mu_0(H + M) \tag{2.2}$$
$$M = \chi H \quad \Rightarrow \quad B = \mu_0(1+\chi)H \tag{2.3}$$
$$\mu_r = 1 + \chi \quad \Rightarrow \quad B = \mu_0 \mu_r H \tag{2.4}$$

However, when using magnetic materials, μ_r is not a constant and so:

$$B = \mu_0(H + M) \tag{2.5}$$

μ_0 is the permeability of free space ($4\pi \times 10^{-7}$ H/m $\approx 1.257 \times 10^{-6}$ H/m),
μ_r is the relative permeability of the material.
M is the magnetisation of the core material.
χ is the volume magnetic susceptibility

By using different materials within the centre of the solenoid different values of mu are used resulting in different hysteresis loops being formed. These B and H values cannot be measured directly. But if you arrange 2 solenoids as in (**Figure 3**).

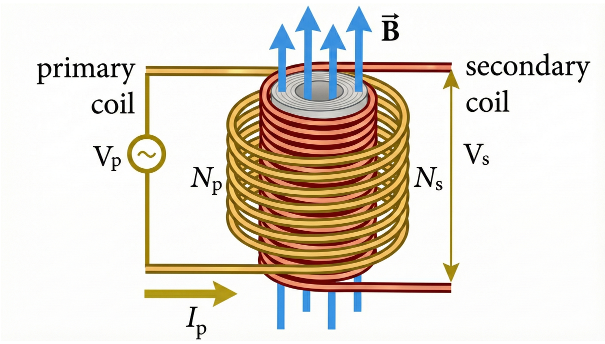

Figure 3: Interlinked solenoids [?].

the variance of the magnetic field in one (the primary solenoid) results in an induced emf in the other coil. This is given by Faraday's law of induction:

$$\mathcal{E} = -N_s \frac{d\Phi}{dt} \tag{2.6}$$

Where: $\mathcal{E}$ is the emf induced in the secondary coil N_s is the number of turns of coil And $\frac{d\Phi}{dt}$ is the rate of change of flux
Φ, the magnetic flux given by:

$$\Phi = BA_s \tag{2.7}$$

Where B is the magnetic flux density inside the coil and is provided by the primary coil and A_s is the area of the secondary coil.

A_s is the Crossectional area of the material in the core.

This secondary coil then allows us to calculate B by integrating $\mathcal{E} = -N_s \frac{d\Phi}{dt}$ to give:

$$B = -\frac{1}{N_s A_s} \int \mathcal{E} dt \tag{2.8}$$

Then through the use of an integrator circuit we can let $V_{out} = -\frac{1}{R_i C} \int \mathcal{E} dt$ and then calculate B using:

$$B = -\frac{R_i C}{N_s A_s} V_{out} \tag{2.9}$$

Our loop allows us to calculate the energy loss per unit volume per cycle from the area under the B-H curve.

$$\frac{P_{\text{loss}}}{V} = f \int H \, \mathrm{d}B, \tag{2.10}$$

Where f is the frequency of the applied magnetic field.
This power loss is mainly due to two effects: hysteresis loss and eddy current loss. Hysteresis loss is the energy dissipated due to the lagging of the magnetic domains behind the applied field, while eddy current loss is due to circulating currents induced in the material by the changing magnetic field.

Further, μ_r values at different points on the curve can be calculated as linear dependence is assumed in the localised region.

$$\mu_r = \frac{1}{\mu_0} \frac{dB}{dH} \tag{2.11}$$

3 Experimental Methods

3.1 Coil assembly and primary circuit

Two coils, one of $\sim$ 500 turns and one of $\sim$ 400 turns, were co-axially wound into a solenoid. The coil with 500 turns was designated the primary coil and connected in series with a $2 \pm 0.1\,\Omega$ resistor (R_p) to reduce the current. This allowed us to calculate the current through the coil and thus the magnetic field strength through the coil ($I = \frac{V}{R_p} \to H = \frac{nI}{L}$, see Equation (2.1)) and ensured the coil did not overheat. This part of the circuit was completed by connecting it to a signal generator set to produce an AC voltage of $5 \pm 0.01 V_{pp}$ (Peak to Peak) at $50 \pm 0.1\,\text{Hz}$ (to emulate mains electricity supply).

The secondary coil was then attached to an integrator circuit.

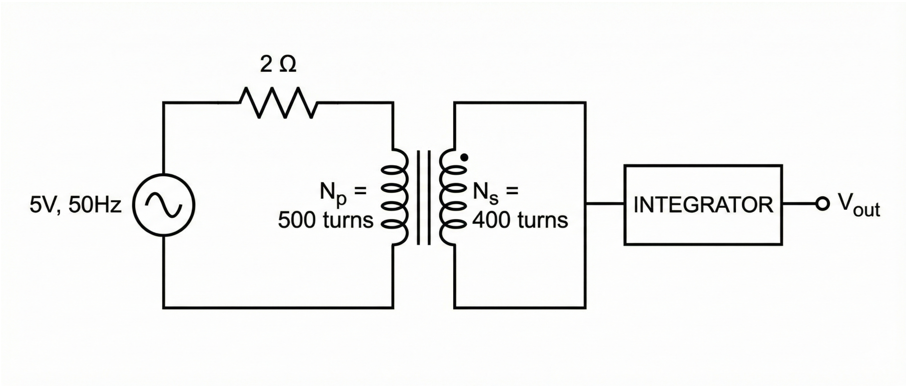

Figure 4: integrator circuit.

3.2 Integrator design and calibration

The integrator circuit was set up as shown below:

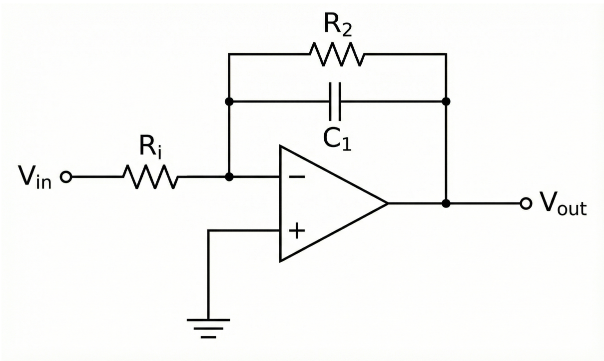

Figure 5: integrator circuit[?].

R_2 was chosen to be, 1MΩ.
After measuring R_2, it was found to be 991.2±0.1$K\Omega$
The value of C_1 s chosen such that $Z_i << 1M\Omega$ at 50 Hz.

$$Z_i << 1M\Omega \tag{3.1}$$
$$Z_i = \frac{1}{\omega C_1} \tag{3.2}$$
$$\frac{1}{\omega C_1} << 1M\Omega \tag{3.3}$$
$$\frac{1}{2\pi \times 50 \times C_1} << 10^6 \tag{3.4}$$
$$C_1 >> 3.18nF \tag{3.5}$$

Therefore Picking 100 nF was suitable.
Next R_i needed to be chosen. To make the calculations easier, an R_i value that would give a

gain of 1 was chosen.

$$gain = \left|\frac{V_{out}}{V_{in}}\right| = \frac{1}{\omega R_i C_1} \tag{3.6}$$

$$1 = \frac{1}{\omega R_i C_1} \tag{3.7}$$

$$R_i = 31.83 K\Omega \tag{3.8}$$

$$R_i \approx 30 K\Omega \tag{3.9}$$

the chosen resistor and capacitor were then measured accurately, Giving:

$$R_i = 32,830 \pm 5\Omega \tag{3.10}$$

$$C_1 = 97.8 \pm 0.1 nF \tag{3.11}$$

$$\therefore$$

$$theoretical\ gain = \frac{1}{2\pi \times 50 \times 32,830 \times 97.8 \times 10^{-9}} = 0.9913 \tag{3.12}$$

After setting up the circuit, the oscilloscope was attached to the signal generator to measure the input and to measure the output of the circuit.

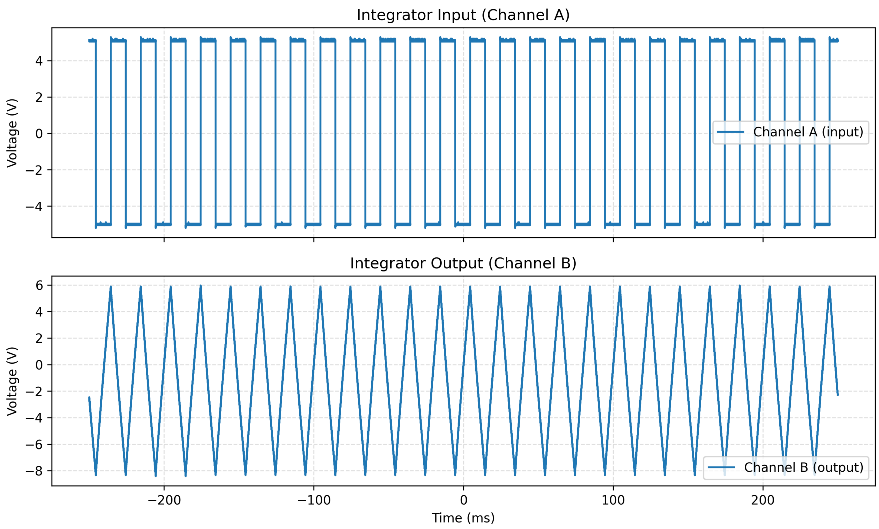

Figure 6: Measurements of the input and output of the circuit figure.

$$Measured\ gain = \left|\frac{V_{out}}{V_{in}}\right| = \frac{14.38V}{10.49V} = 1.37 \pm 0.005 \tag{3.13}$$

This is a 38% deviation from the theoretical value and may be due to a square wave being tested. This is composed of sinusoidal waves of many frequencies and so will have some at the odd harmonics of the fundamental frequency of the integrator circuit (e.g. 3f = 150 Hz, 5f = 250 Hz, etc.). This is combined with the op-amp not being ideal and having a limited bandwidth can result in a different gain to the theoretical value. This is treated as a systematic error in the experiment and was used as gain in the subsequent calculations.

3.3 Data acquisition and sample preparation

The samples used were:
• Mild steel
• Transformer iron
• CuNi alloy at 10°C and above 40°C

the coil length and the cross-sectional area of the samples were measured. This was done using a vernier caliper to measure the length and width of the cuboid CuNi alloy and transformer iron samples and the diameter of the cylindrical mild steel sample.
Then the experiment was run: The signal generator was turned on to feed an AC current into the primary coil after Waiting until the circuit reached a steady state the data points for 20 cycles were saved. This was done immediately to ensure the coil didn't heat up and change its resistance during the measurement. The coil was then turned off and this was repeated for the other samples.

First the measurements were performed without a sample (air) to act as a control, then metals.

When measuring the CuNi alloy it was placed into hot water to raise its temperature to above 40°C and then placed into ice water to cool it to 10°C. The low time difference between the samples being removed from the water and being tested results in minor temperature changes during the measurement but the actual temperature was not measured during the hysteresis and thus the temperatures should be taken as approximate.

Voltages across the series 2 Ω resistor (Channel A) and integrator output (Channel B) were recorded using a PicoScope at a sampling rate of 1.95 MHz (in spite of the AC current being used the PicoScope was set to DC. This was to avoid the possibility of some AC current being filtered out by the PicoScope as it is seen as DC offset as a result of the low frequency being used). For each sample 20 cycles at 50 Hz (∼0.32 s) were recorded. Was then exported to be analysed using a Python script that splits up the individual loop and plots them for a visual check during the experiment and allowed for further analysis later in Section 4.

4 Results and Analysis

4.1 Overview

The first step was to record the nominal measurements of the samples used throughout the run, which are summarised in Table 1 below. Over the course of the experiment five sets of data were collected:

•the air control experiment
•mild steel,
•transformer iron
•CuNi alloy at approximately 10 °C
•CuNi alloy at 40 °C

The transformer iron and elevated-temperature CuNi alloy datasets were each recorded twice; the repeats agreed with the original measurements within the random scatter, so only the original runs are used in the tables below.

Table 1: Nominal sample dimensions and cross-sectional areas used to convert the voltage measurements into magnetic quantities.

Sample	Key measurements	Cross-sectional area (mm^2)
Air control	Diameter = 7.8 ± 0.1 mm	47.8 ± 1.2
Mild steel	Diameter = 3.12 ± 0.04 mm	7.65 ± 0.2
Transformer iron	width = 4.22 ± 0.02 mm, Thickness = 0.7 ± 0.02 mm	2.95 ± 0.16
Copper Nickel alloy	Diameter = 5.00 ± 0.02 mm	19.6 ± 0.16

Twenty loops of the steady-state response were recorded for each dataset. Using Equations (2.1) and (2.9), the voltages across the 2 Ω resistor and the integrator output were converted into magnetic field strength H and magnetic flux density B for the plots that follow.

From the multiple recorded loops, the mean and standard deviation of key metrics were calculated and used as estimates of random uncertainties. In all cases, loop-to-loop scatter was small. Larger systematic uncertainties are expected from calibration of the integrator gain, resistor values and sample geometry; these are not included in the quoted error bars but are discussed qualitatively in Section 5

4.2 Air calibration

The air control plot shows the expected linear response with no hysteresis, because the permeability should be close to that of free space. The behavior was modelled by $B = \mu_0 \mu_r H$, and the apparent relative permeability μ_r calculated from the slope is smaller than the expected value. The error in the fitted line does not account for this offset, so the discrepancy is interpreted as a systematic error possibly due to parasitic capacitance.

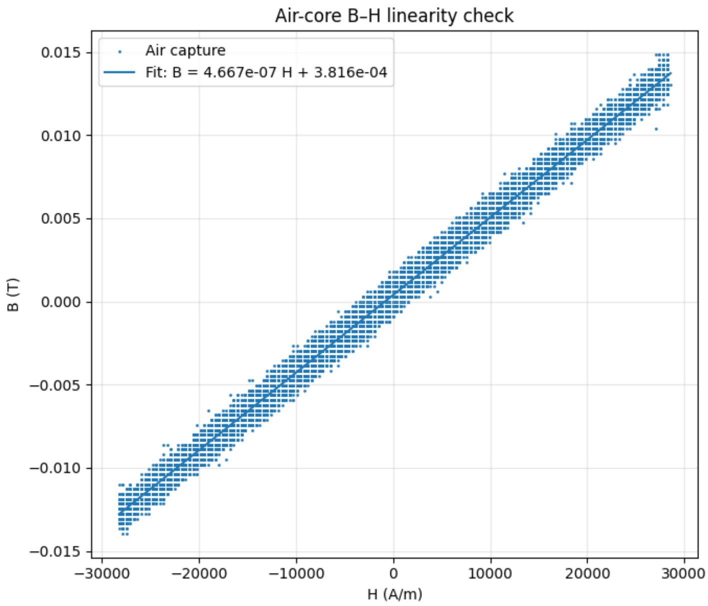

Figure 7: Linear $B(H)$ response obtained from the air control experiment.

the figure 7 shows a strong linear response from the air control experiment as expected. there is minor scatter between the loops which is likely due to noise in the measurement system. This resulted in the low uncertancy calcuated using the standard deviation between gradients and intercepts in the set of modeled loops.

Interpreting the results from 7, the relative permeability μ_{r} was calculated from the numeric gradient dB/dH.

$$\mu_{\mathrm{r}} = \frac{1}{\mu_0}\frac{dB}{dH} \tag{4.1}$$

$$y = (4.667 \times 10^{-07} \pm 1.260 \times 10^{-10})x + (3.816 \times 10^{-04} \pm 2.511 \times 10^{-06}) \tag{4.2}$$

$$\therefore$$

$$\mu_{\mathrm{r}} = 0.37 \pm 0.03 \tag{4.3}$$

This value is significantly lower than the expected $\mu_{\mathrm{r}} \approx 1$ for air, indicating a systematic error in the measurement setup.

4.3 Hysteresis plots

the 20 recorded hysteresis loops for each material were plotted individually. In all three ferromagnetic datasets the raw $B(H)$ loops show small secondary loops at large $|H|$ (most clearly in transformer iron, Figure 10).
To account for this the end tails of the hysteresis loops were fitted to fifth order polynomials allowing a smooth gradient to be found at the ends, allowing us to give a more stable estimate of the saturation permeability.

4.3.1 Mild steel

Figure 8 shows the raw hysteresis data for the mild steel sample.

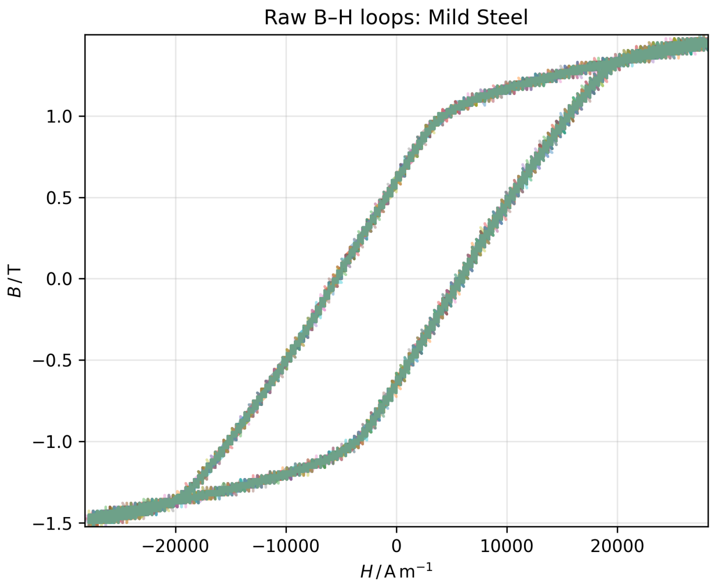

Figure 8: Raw mild steel hysteresis loops.

After applying the fifth-order polynomial fit to the tails, we obtained the smoother loop shown in Figure 9.

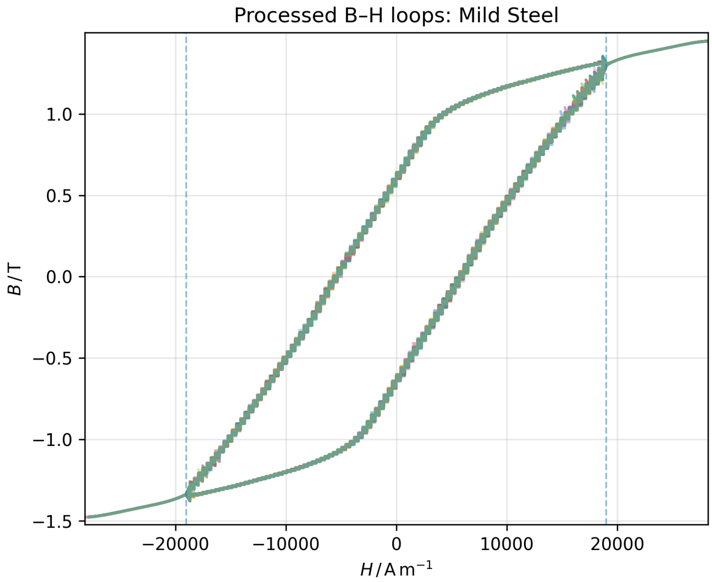

Figure 9: Mild steel hysteresis loop after polynomial tail fitting.

The processed loop (figure 9) shows relatively wide hysteresis curve with a saturation flux density of around 1.4T and a coercive field in the order of 10^3 Am^{-1}

Table 2: Mild steel loop statistics from the polynomial-tail analysis (cell 10 of the notebook).

Quantity	Value	Uncertainty	Units
B range	2.92	0.00034	T
H range	5.61×10^4	31	Am^{-1}
Power loss per unit area	1.38×10^6	410	$\mathrm{W\,m}^{-3}$
Maximum μ_r (numeric gradient)	123	4.5	—
Minimum μ_r (numeric gradient)	14.0	0.025	—

4.3.2 Transformer iron

Figure 10 shows the raw transformer iron loops, which also required polynomial smoothing of the tails.

The transformer iron loop (Figure 11) is narrower and steeper in the central region than for mild steel, with a similar saturation flux density but a smaller coercive field.

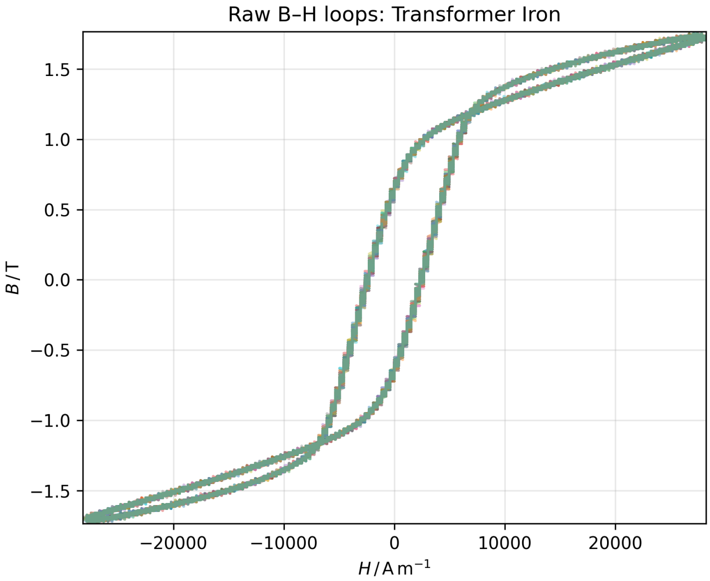

Figure 10: Raw transformer iron hysteresis loops.

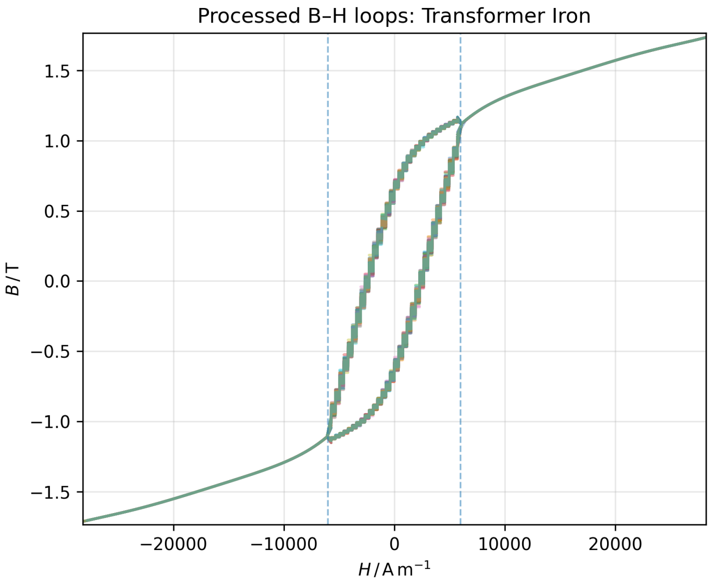

Figure 11: Transformer iron loop after polynomial tail fitting.

Table 3: Transformer iron loop statistics from the polynomial-tail analysis (cells 7 and 9).

Quantity	Value	Uncertainty	Units
B range	3.44	0.00068	T
H range	5.61×10^4	38	$\mathrm{Am^{-1}}$
Power loss per unit area	4.73×10^5	1050	$\mathrm{W\,m^{-3}}$
Maximum μ_r (numeric gradient)	332	4.2	—
Minimum μ_r (numeric gradient)	13.9	0.025	—

4.3.3 CuNi at 10 °C

The CuNi alloy at 10 °C follows similar behaviour, with the raw data plotted in Figure 12.

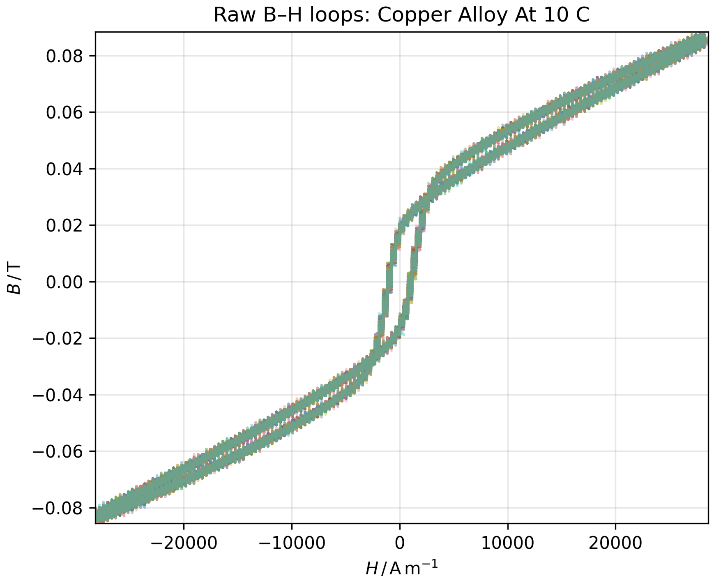

Figure 12: Raw CuNi (10 °C) hysteresis loops.

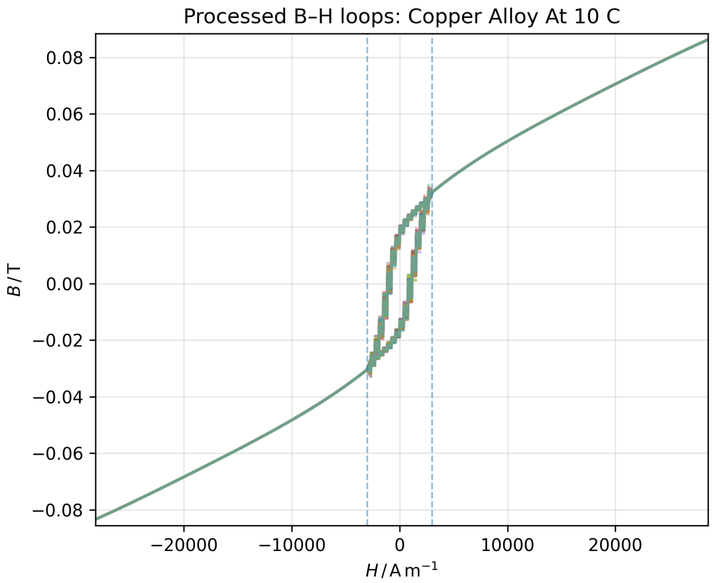

Figure 13: Polynomial-fit CuNi (10 °C) loop.

At 10 °C the CuNi alloy still shows a small but clear hysteresis loop (Figure 13), but the b range of only 0.17 ± 0.01 T is about 20 times smaller than for transformer iron, and the loop is much narrower in H.

Table 4: CuNi (10 °C) loop statistics after polynomial tail smoothing (cell 11).

Quantity	Value	Uncertainty	Units
B range	0.17	0.00001	T
H range	5.68×10^4	1.7×10^{-12}	$\mathrm{Am^{-1}}$
Power loss per unit area	4605	20.5	$\mathrm{W\,m^{-3}}$
Maximum μ_r (numeric gradient)	7.88	0.0023	—
Minimum μ_r (numeric gradient)	1.35	0.0037	—

4.3.4 CuNi at 40 °C

Heating the CuNi sample to 40 °C suppresses the hysteresis, leaving a near-linear $B(H)$ response (Figure 14). A linear regression therefore replaced the polynomial tail fits for this dataset.

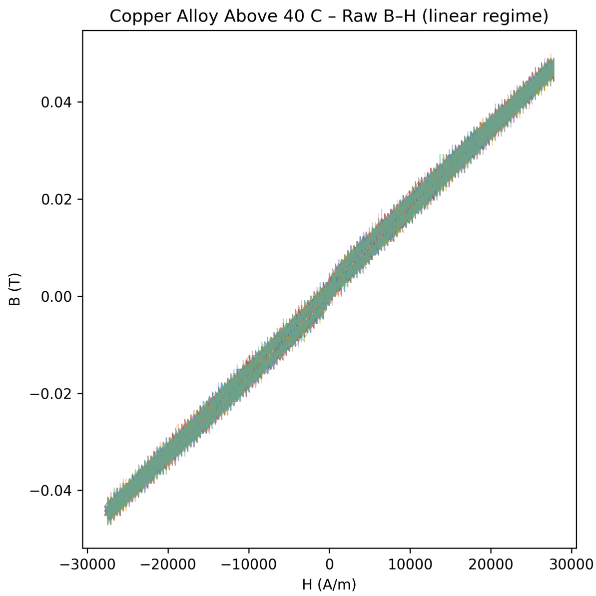

Figure 14: Raw CuNi (40 °C) data showing the predominantly linear response.

When the CuNi alloy is heated to 40 °C, the loop collapses into an almost straight line (Figure 15). Within the scatter, the data are consistent with a single linear relation $B = B_0 + (1.67 \pm 0.03) \times 10^{-6} H$, corresponding to an effective $\mu_r = 1.33 \pm 0.01$.

This is consistent with the alloy being just above its Curie temperature, where the material is only weakly paramagnetic and shows negligible hysteresis.

Table 5: Linear regression summary for CuNi at 40 °C (cell 13).

Quantity	Value	Uncertainty	Units
B range	0.0954	0.00011	T
H range	5.56×10^4	19	$\mathrm{Am^{-1}}$
Slope dB/dH	1.67×10^{-6}	3.36×10^{-10}	$\mathrm{TA^{-1}m^{-1}}$
Intercept B_0	0.00108	6.58×10^{-6}	T
Relative μ_r (linear fit)	1.33	7.2×10^{-5}	—

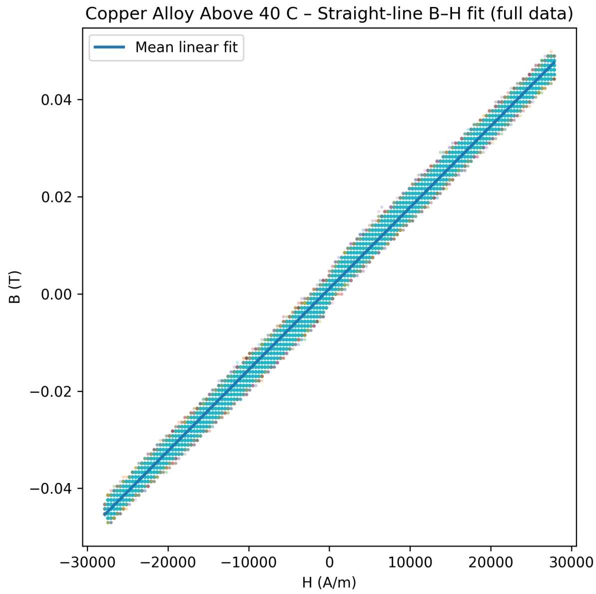

Figure 15: Linear regression for the CuNi (40 °C) run.

4.4 Summary of results

Table 6: Summary of the collected data sets.

Data set	Notes
Air control experiment	Baseline linear response, no hysteresis expected.
Mild steel	Hysteresis loop with pronounced end tails.
Transformer iron	Initial loop deviated from literature; repeated run matched original.
Copper at 10 °C	Hysteresis loop with tail artefacts.
Copper at 40 °C	Repeat confirmed the linear response with negligible hysteresis.

Table 7 collects each sample's peak and minimum μ_r together with the power loss per unit area so the datasets can be compared directly.

Table 7: Aggregated magnetic metrics across the measured trials.

Sample	Max μ_r	Min μ_r	Power loss per unit area ($\mathrm{W\,m^{-3}}$)
Mild steel	123	14.0	1.38×10^6
Transformer iron	332	13.9	4.73×10^5
CuNi (10 °C)	7.88	1.35	4605
CuNi (40 °C)	1.33	1.33	6300

Comparing the samples, transformer iron has the largest maximum permeability ($\mu_{r,\max} \approx 332$) and the smallest hysteresis loss ($\sim 5 \times 10^5\ \mathrm{W\,m^{-3}}$), making it the most suitable transformer-core material among those tested. Mild steel also has a relatively high μ_r but suffers from much larger hysteresis losses. The CuNi alloy has much lower μ_r and loss; at 10 °C it shows a small hysteresis loop, while by 40 °C it behaves almost linearly with $\mu_r \approx 1.3$, i.e. only slightly different from air.

5 Discussion

6 Conclusion

References

[1] Robert Keim. What is hysteresis? an introduction for electrical engineers, 2023.

[2] Hysteresis loop, 2025.